Exchange of Histidine Spacing between Sp1 and GLI Zinc Fingers: Distinct Effect of Histidine Spacing-Linker Region on DNA Binding†

Yasuhisa Shiraishi, Miki Imanishi, and Yukio Sugiura*

Institute for Chemical Research, Kyoto University, Uji, Kyoto 611-0011, Japan

Received November 9, 2003; Revised Manuscript Received March 12, 2004

ABSTRACT: In the DNA recognition mode of C_2H_2-type zinc fingers, the finger−finger connection region, consisting of the histidine spacing ($HX_{3-5}H$) and linker, would be important for determining the orientation of the zinc finger domains. To clarify the influence of spacing between two ligand histidines in the DNA binding, we exchanged the histidine spacing between Sp1 and GLI zinc fingers, which have an HX_3H-TGEKK linker (typical) and an HX_4H-SNEKP linker (atypical), respectively. A significant decrease in the DNA binding affinity and specificity is found in Sp1-type peptides, whereas GLI-type peptides show a mild reduction. To evaluate the effect of the linker characteristics, we further designed Sp1-type mutants with an SNEKP linker. As a result, the significant effect of the histidine spacing in Sp1-type peptides was reduced. These results demonstrate that (1) the histidine spacing significantly affects the DNA binding of zinc finger proteins and (2) the histidine spacing and the following linker regions are one effective target for regulating the DNA recognition mode of zinc finger proteins.

A C_2H_2-type zinc finger has a tandemly repeated structure, which consists of independent modules with the consensus sequence (Tyr, Phe)-X-Cys-$X_{2,4}$-Cys-X_3-Phe-X_5-Leu-X_2-His-X_{3-5}-His-X_{2-6}. Each domain forms a compact $\beta\beta\alpha$ structure held together tetrahedrally by coordination of a zinc ion with two invariant cysteines and histidines. Typical C_2H_2-type zinc fingers recognize the three-base-pair subsite mainly on one strand using key amino acid residues of the α-helix (*1*, *2*). On the basis of these features, new zinc fingers with various sequence specificities have been designed by mutating amino acid residues in the α-helix by rational structural design (*3*−*6*) and by a phage-display-based method (*7*−*11*). To expand the DNA recognition mode of zinc finger proteins, two significant factors should be considered: (i) the base recognition on the complementary DNA strand overlaps the DNA recognition of the preceding zinc finger (*12*, *13*), and (ii) the orientation of each zinc finger is restricted by the structure of the finger−finger connection region consisting of a histidine spacing and a linker (*14*). In this study, we focus on the influence of the histidine spacing for the DNA binding. The histidine spacing is conserved from HX_3H to HX_5H and has various conformations in accordance with the number of amino acid residues. On the basis of the previous structural analyses, an HX_3H-type spacing forms a 3_{10}-helix, whereas HX_4H-type and HX_5H-type spacings form helical structures (*15*, *16*). The local conformational alteration of the histidine spacing might result in changing the DNA binding of zinc finger proteins. To evaluate the influence of the histidine spacing on the DNA binding, we selected HX_3H-type and HX_4H-type spacings, because these are the most common motifs in nature. The Sp1 zinc finger has a typical DNA recognition mode and structure found in many C_2H_2-type zinc fingers, and hence it was chosen as an HX_3H-type zinc finger (*17*−*19*). On the other hand, we determined the GLI zinc finger as an HX_4H-type zinc finger from the following reasons: (i) there are unique HX_4H-type zinc fingers such as Tramtrack and TFIIIA, but these zinc fingers have distinct linker length from the TGEKP linker (*20*, *21*), and (ii) the GLI zinc finger has been well studied structurally and functionally, and it shares the appreciably similar amino acid sequences in the histidine spacing with the Sp1 zinc finger (*22*, *23*).

Human transcription factor Sp1 is a sequence-specific DNA binding protein and has three continuous repeats of a C_2H_2-type zinc finger at the C-terminal region (*17*, *18*). Each zinc finger motif involves an HX_3H-type spacing and a typical TGEKK linker. The previous studies revealed that the C-terminal two fingers of Sp1, Sp1(zf23), show a typical binding mode (*19*). On the other hand, the GLI oncogene encodes five repeated C_2H_2-type zinc fingers, and its C-terminal two fingers, GLI(zf45), have HX_4H motifs and an atypical SNEKP linker (*22*). The crystal structure of the GLI−DNA complex demonstrated that GLI(zf45) makes contact with the extensive 10 bp on both DNA strands (*23*). In this study, we converted the HX_3H-type spacing of Sp1(zf23) into the HX_4H-type spacing of GLI(zf45) and vice versa. The alterations of the DNA binding affinity and the DNA binding mode by these new zinc finger peptides were investigated, and the effect of the histidine spacing and the following linker has been discussed.

MATERIALS AND METHODS

Chemicals. The T4 polynucleotide kinase and restriction enzymes were purchased from New England Biolabs. Taq DNA polymerase and synthesized oligonucleotides for clon-

† This study was supported in part by Grants-in-Aid for COE Project Element Science (12CE2005) and Scientific Research (13557210• 14370755) from the Ministry of Education, Culture, Sports, Science, and Technology, Japan. Y.S. is a research fellow of the Japan Society for the Promotion of Science.

* To whom correspondence should be addressed. Phone: +81-774-38-3210. Fax: +81-774-32-3038. E-mail: sugiura@scl.kyoto-u.ac.jp.

10.1021/bi035999s CCC: $27.50
Published on Web 04/23/2004

ing each peptide were acquired from Qiagen and SIGMA GENOSYS, respectively. Labeled compound [γ-^{32}P]ATP was supplied by DuPont. The plasmid pBS-Sp1-fl was kindly provided by Dr. R. Tjian. All other chemicals were of commercial reagent grade.

Preparations of Zinc Finger Peptides and Substrate DNA Fragments. Sp1(zf123) and Sp1(zf23), the aliases for Sp1(530−623) and Sp1(566−623), are coded on the plasmids pEVSp1(530−623) and pEVSp1(566−623), respectively, as previously described (*24*). All other peptides were created by a standard polymerase chain reaction with the appropriate primer sets using pEVSp1(530−623) or pEVSp1-(566−623) as templates. Their sequences were confirmed by a GeneRapid DNA sequencer (Amersham Biosciences). These zinc finger peptides were overexpressed as a soluble form in *Escherichia coli* strain BL21(DE3)pLysS at 25 °C and purified by the following procedure at 4 °C. *E. coli* cells were resuspended and lysed in PBS buffer. After centrifugation, the supernatant containing the soluble form of the zinc finger peptides was purified by cation-exchange chromatography using a 0.05−2.0 M NaCl gradient (Mono S HR 5/5; Amersham Biosciences). Final purification was achieved by a gel filtration technique (Superdex 75; Amersham Biosciences) using TN[1] buffer [10 mM Tris-HCl (pH 8.0), 50 mM NaCl, and 1 mM dithiothreitol]. For preparing the substrate DNAs, oligonucleotides containing the GC box sequence or the GLI binding sequence were provided (GC1, 5′-GATCTGGGGCGGGGCCT-3′; GC2, 5′-AATTAGGCCCCGCCCCA-3′; GLI1, 5′-GATCTCGTGGACCACCCAAGACGAAT-3′; and GLI2, 5′-AATTATTCGTCTTGGGTGGTCCACGA-3′). The complementary oligonucleotides were annealed and inserted between a *Bam*HI site and an *Eco*RI site of pBluescript II SK+ (Stratagene, La Jolla, CA). The *Hin*dIII−*Xba*I fragments (GC box, 41 bp, and GLIseq, 50 bp, respectively) were cut out and labeled at the 5′-end with ^{32}P for the experiments as described previously (*5*).

CD Measurements. The CD spectra for all of the zinc finger peptides were recorded on a Jasco J-720 spectropolarimeter in 10 mM Tris-HCl (pH 8.0), 50 mM NaCl, 1 mM dithiothreitol, and 10 μM zinc finger peptide at 20 °C.

Gel Mobility Shift Assays. Gel mobility shift assays were carried out under the previous experimental conditions (*25*). Each reaction mixture contained 10 mM Tris-HCl (pH 8.0), 50 mM NaCl, 1 mM dithiothreitol, 10 μM $ZnCl_2$, 25 ng/μL poly(dI-dC), 0.05% Nonidet P-40, 5% glycerol, 800 μg/mL bovine serum albumin, the ^{32}P-end-labeled substrate DNA fragment (∼50 pM, 500 cpm), and 0−4 μM zinc finger peptide. After incubation at 20 °C for 30 min, the sample was run on an 8% polyacrylamide gel with 89 mM Tris−borate buffer at 20 °C. The bands were visualized by autoradiography and quantified with ImageMaster 1D Elite software (version 3.01). The dissociation constants (K_d) of the Sp1 and GLI peptide−DNA fragment complexes were estimated according to the previously reported procedure (*24*).

DNase I Footprinting Analyses. DNase I footprinting experiments were performed according to the method of Brenowitz et al. (*26*). The binding mixture contained 20 mM Tris-HCl (pH 8.0), 25 mM NaCl, 5 mM $CaCl_2$, 10 mM $MgCl_2$, 20 ng/μL sonicated calf thymus DNA, the 5′-end-labeled substrate DNA fragment (∼6 nM, 30 kcpm), and 0−8 μM peptide. To show the evident footprinting patterns, we selected the maximum protein concentration rather than the concentration near the K_d values in DNase I footprinting analyses. We conducted the preliminary gel mobility shift assays with the same reaction buffer as DNase I footprinting (except for addition of glycerol) and determined the maximum protein concentration. After incubation at 20 °C for 30 min, the sample was digested with DNase I (0.5 milliunit/μL) at 20 °C for 2 min. The reaction was stopped by the addition of 20 μL of DNase I stop solution (0.1 M EDTA and 0.6 M sodium acetate) and 100 μL of ethanol. After ethanol precipitation, the cleavage products were analyzed on a 15% polyacrylamide/7 M urea sequencing gel. The bands were visualized by autoradiography.

Methylation Interference Analyses. The recognition of guanines in the primary and secondary strands of the GC box (the G- and the C-strands, respectively) by each peptide was investigated by methylation interference assays as described previously (*27*). The binding reaction mixture contained 10 mM Tris-HCl (pH 8.0), 50 mM NaCl, 1 mM dithiothreitol, 10 μM $ZnCl_2$, 25 ng/μL poly(dI-dC), 0.05% Nonidet P-40, 5% glycerol, 800 μg/mL bovone serum albumin, the ^{32}P-end-labeled methylated DNA fragment (∼60 nM, 500 kcpm), and 20−750 nM zinc finger peptide. After incubation at 20 °C for 30 min, the peptide-bound and free DNAs were separated on a 10% nondenaturing polyacrylamide gel and eluted from the gel with a standard elution buffer. To examine both the strong and weak base contacts, we selected the experimental conditions under which the ratio of peptide−DNA complexes to total probes is about 10−20%. The recovered methylated DNA was reacted in 100 μL of 1 M piperidine at 90 °C for 30 min. The lyophilized cleavage products were analyzed on a 15% polyacrylamide/7 M urea sequencing gel. The bands were visualized by autoradiography and quantified with ImageMaster 1D Elite software (version 3.01). The extent of interference was estimated for each base by calculating the ratio of the cutting probabilities in the free and bound lanes.

RESULTS

Designs of Zinc Finger Peptides and Substrate DNAs. Figure 1A shows the putative base recognition mode of the Sp1 zinc finger (*24*), and Figure 1B exhibits the recognition mode of the C-terminal two fingers of GLI determined by X-ray structural analysis (*23*). In pursuit of the effect of the histidine spacing on the DNA binding, we designed several zinc finger peptides based on Sp1(zf23) and GLI(zf45). All of the peptides used in this study are summarized in Figure 1C. We prepared four two-finger-type and six three-finger-type peptides. Sp1(zf23)HX_4H and GLI(zf45)HX_3H were designed by exchanging their histidine spacing. In addition, we examined the effect on the DNA binding of the total Sp1 zinc finger domain by preparing Sp1(zf123)HX_4H, in which the N-terminal zinc finger (finger 1) of Sp1 is connected to Sp1(zf23)HX_4H. Sp1(SNE) and Sp1(SNE)HX_4H were designed by substituting an SNEKP linker for a TGEKK linker to investigate the effect of the linker. To evaluate the effect on finger 1, we prepared Sp1(KA) or Sp1(KA)HX_4H, in which lysine at the helical position −1 of finger 1 in Sp1(zf123) or Sp1(zf123)HX_4H was substituted with alanine.

[1] Abbreviations: Tris, tris(hydroxymethyl)aminomethane; TN, Tris−NaCl; CD, circular dichroism; zf, zinc finger; bp, base pair(s).

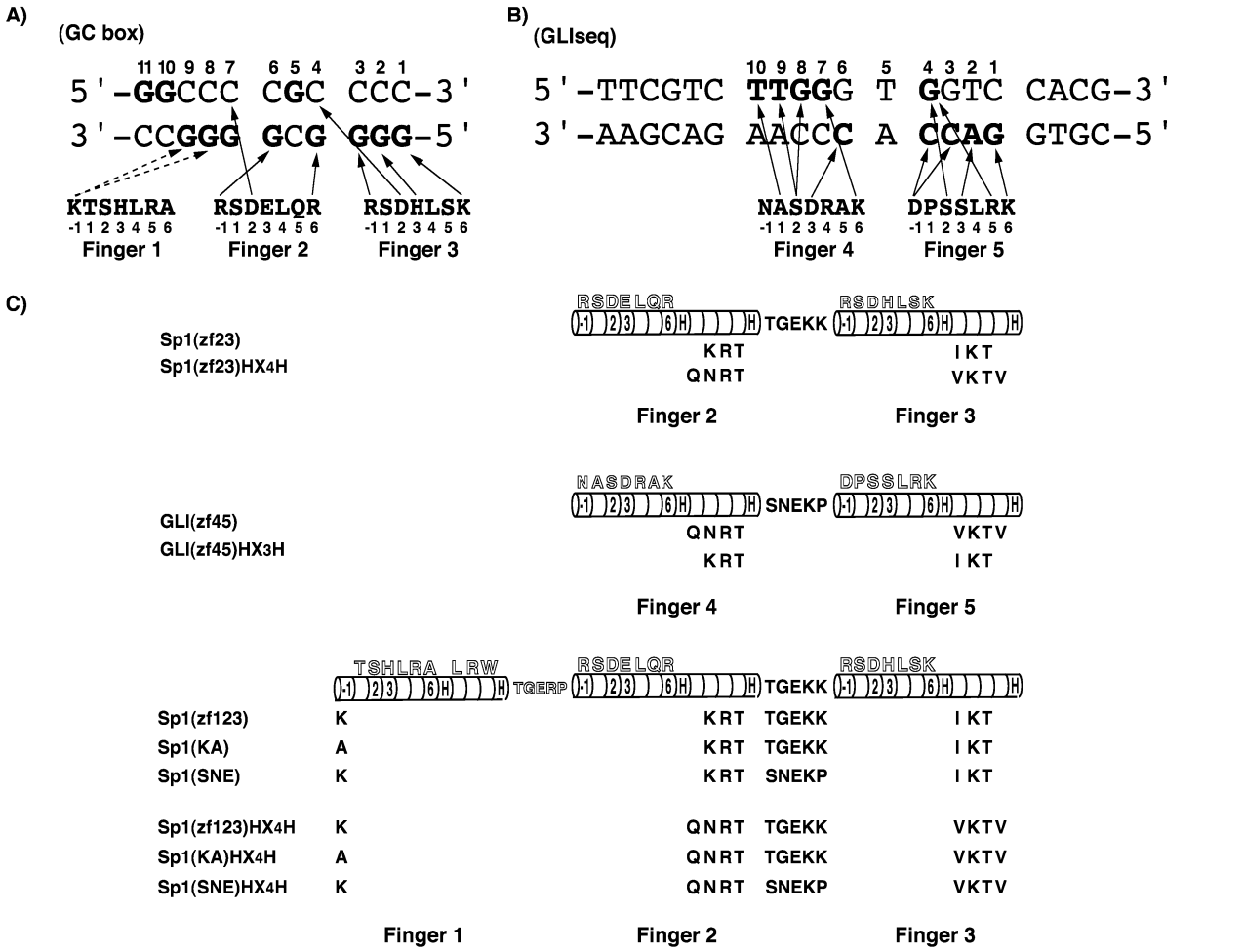

FIGURE 1: (A) Putative base recognition mode of three zinc fingers of Sp1. Amino acid residues at the N-terminus of the α-helix in each finger are depicted by their one-letter codes with the number of the helical positions below. Solid arrows show the amino acid−base contacts assumed by the DNA binding mode of Zif268, and dotted arrows depict the contacts indicated by our previous report (*24*). The guanine bases, whose methylation interferes with the zinc finger binding, are in bold print. (B) Established base recognition mode of the C-terminal two zinc fingers of GLI by crystal structure (*23*). Solid arrows show the base recognition, and the bases recognized by amino acids are written in bold characters. (C) Primary structures of two-finger-type and three-finger-type zinc finger peptides. The designation of each zinc finger is shown by the original name (fingers 1−3 and 4−5). The amino acid residues in the linker and the α-helix of each peptide are indicated by their one-letter codes, and the mutated residues are in bold print.

It is well-known that this lysine contributes to the base recognition and the DNA binding affinity of the Sp1 zinc finger (*24*).

Two types of substrate DNA were prepared. The GC box is the substrate for the Sp1-type zinc finger derived from the mouse dihydrofolate reductase promoter (I and III) (*24*). The GLIseq is the substrate derived from the X-ray structure of the GLI−DNA complex, containing the consensus sequence for the binding of the GLI zinc finger (*23*).

CD Features of HX_3H-Type and HX_4H-Type Zinc Finger Peptides. The folding properties of the present peptides were evaluated by measurements of the CD spectra. Figure 2 shows the CD spectra of the peptides at 20 °C. The spectrum for Sp1(zf23) was similar to those for the single- and three-finger peptides of Sp1 described previously (*13*, *28*, *29*). Negative Cotton effects in the far-UV region with a minimum around 208 nm and a shoulder around 222 nm suggest that all of the two-finger peptides have ordered secondary structures with helical conformation. However, the HX_4H-type peptides exhibited CD spectra different from those of the HX_3H-type peptides, especially in the ellipticities at 222 nm. The values of Sp1(zf23)HX_4H ([θ] = −9653) and

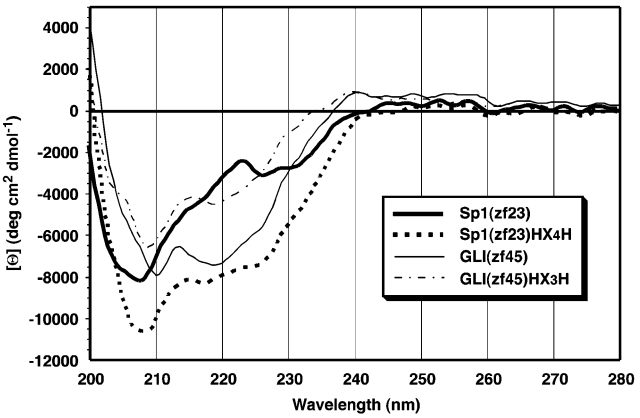

FIGURE 2: CD spectra of two-finger-type zinc finger peptides of Sp1 and GLI at 20 °C. Respective zinc finger peptides are indicated in the figure.

GLI(zf45) ([θ] = −6739) were larger than those of Sp1(zf23) ([θ] = −3840) and GLI(zf45)HX_3H ([θ] = −4325). Sp1(zf123) and Sp1(zf123)HX_4H also showed the spectral patterns similar to those of Sp1(zf23) and Sp1(zf23)HX_4H (data not shown). In general, the ellipticities at 222 nm

Table 1: Apparent Dissociation Constants (K_d) for Sp1(zf23) and Sp1(zf23)HX_4H Binding to the GC Box and for GLI(zf45) and GLI(zf45)HX_3H Binding to the GLIseq

binding site[b]	K_d (nM)[a]			
	Sp1(zf23)	Sp1(zf23)HX_4H	GLI(zf45)	GLI(zf45)HX_3H
GC box	3.4 ($\pm$0.2) $\times$ 10^2	ND[c]		
GLIseq			3.8 ($\pm$0.3) $\times$ 10^2	8.3 ($\pm$0.3) $\times$ 10^2

[a] Apparent dissociation constants were determined by titration using gel mobility shift assays as described in Materials and Methods. Values are averages of three or more independent determinations with standard deviations. [b] The nomenclature is described in the text (see Figure 1). [c] ND represents not determined.

Table 2: Apparent Dissociation Constants (K_d) for Sp1(zf123), Sp1(zf123)HX_4H, Sp1(KA), Sp1(KA)HX_4H, Sp1(SNE), and Sp1(SNE)HX_4H Binding to the GC Box

binding site[b]	K_d (nM)[a]					
	Sp1(zf123)	Sp1(zf123)HX_4H	Sp1(KA)	Sp1(KA)HX_4H	Sp1(SNE)	Sp1(SNE)HX_4H
GC box	1.3 ($\pm$0.1) $\times$ 10	8.4 ($\pm$0.6) $\times$ 10^2	5.5 ($\pm$0.1) $\times$ 10	9.7 ($\pm$1.2) $\times$ 10^2	1.7 ($\pm$0.3) $\times$ 10	1.7 ($\pm$0.1) $\times$ 10^2

[a] Apparent dissociation constants were determined by titration using gel mobility shift assays as described in Materials and Methods. Values are averages of three or more independent determinations with standard deviations. [b] The nomenclature is described in the text (see Figure 1).

indicate the content of α-helix. Therefore, the increase in negative Cotton effects of the HX_4H-type zinc fingers mainly reflects the increase of α-helix content in the histidine spacing observed in the previous report (*15*).

DNA Binding Affinity of Each Zinc Finger Peptide. To evaluate the effect of the histidine spacing on DNA binding affinity, we prepared two types of substrate DNAs (GC box and GLIseq) and determined the apparent dissociation constants (K_d) of each zinc finger peptide for the substrate DNA using gel mobility shift assays (Tables 1 and 2). Sp1(zf23) bound to the GC box with K_d = 340 nM, consistent with the previous result (*24*), whereas Sp1(zf23)HX_4H did not show any shift band even at the maximum concentration. In general, DNA binding proteins including the zinc finger have many basic amino acid residues, and they could bind average sequence DNA with electrostatic force. Sp1(zf23) has lower specificity for the GC box compared with Sp1(zf123), and hence the effect of nonspecific binding is relatively stronger than that of Sp1(zf123). To remove the effect of nonspecific DNA binding, we also determined the K_d values in the absence of nonspecific DNA. The Sp1(zf23)-GC box was approximately 7 nM, while that of Sp1(zf23)HX_4H was over 750 nM (data not shown). We further analyzed the effect on the DNA binding affinities of the three-finger-type zinc fingers of Sp1. The binding affinity of Sp1(zf123) for the GC box (13 nM) was comparable with that in the previous report (*13*). A drastic reduction in binding affinity was also detected in Sp1(zf123)HX_4H (840 nM), and this K_d value was 65-fold higher than that of Sp1(zf123). To evaluate the effect of the exchanged histidine spacing in finger 2 and finger 3 on finger 1 of Sp1, we determined the K_d values of Sp1(KA) (55 nM) and Sp1(KA)HX_4H (970 nM). The 4.2-fold decrease in DNA binding affinity was found in Sp1(KA) compared with Sp1(zf123), whereas the binding affinity of Sp1(KA)HX_4H was only 1.2-fold lower than that of Sp1(zf123)HX_4H. On the other hand, the K_d values of GLI(zf45) and GLI(zf45)HX_3H were 380 and 830 nM, respectively. Accordingly, the effect of the change in the histidine spacing on DNA binding affinity was milder in GLI-type peptides (2.2-fold reduction) than in Sp1-type peptides. The K_d values of Sp1(SNE) (17 nM) and Sp1(SNE)HX_4H (170 nM) were determined for examining the effect of the linker. As a result, Sp1 with an SNEKP linker was less sensitive to the change of the histidine spacing than Sp1 with a TGEKK linker. Of special interest is the fact that the DNA binding affinity of Sp1(SNE)HX_4H is 4.9 times higher than that of Sp1(zf123)HX_4H, while those of Sp1(zf123) and Sp1(SNE) are comparable.

DNA Binding Modes of Zinc Finger Peptides Detected by Footprinting Technique. In general, DNase I footprinting analyses are available for detecting not only peptide binding regions but also conformational changes in the substrate DNA. In experiments of DNA binding proteins, the selection of nonspecific DNAs is important for gaining the correct result. To compare our results with the previous result (*24*), we selected calf thymus DNA in DNase I footprinting analyses. In addition, we also confirmed that the footprinting patterns were not changed between dI-dC and calf thymus DNA. The results of Sp1(zf123) and Sp1(zf123)HX_4H for the G-strand are shown in Figure 3. Because the DNA binding of Sp1(zf23)HX_4H was too weak to detect any protected regions from the DNase I cleavage, three-finger peptides were used for this assay. Sp1(zf123) exhibited protection of the GC box region and upstream of the GC box region, and the hypersensitive cleavage at the 5′-AA-3′ step outside the GC box region in the guanine-rich strand (G-strand) was observed as seen in the previous report (*24*, *25*). On the contrary, Sp1(zf123)HX_4H could not protect the GC box region specifically, and also the hypersensitive cleavage was not detected at all, even at 4 μM. These observations indicate that Sp1(zf123)HX_4H loses the DNA binding mode of Sp1(zf123). Figure 4 shows the DNase I footprinting patterns of GLI(zf45) and GLI(zf45)HX_3H for GLIseq. GLI(zf45) protected the region containing the expected 10 bp binding site of the C-terminal two fingers of the GLI zinc finger in strands (i) (Figure 4A) and (ii) (Figure 4B), indicating that the unique binding mode of the GLI zinc finger is probably maintained even in GLI(zf45). GLI(zf45)HX_3H also protected the same position in strand (ii) as GLI(zf45). Although the footprinting pattern of GLI(zf45)HX_3H was not so evident in strand (i), both GLI-type variants showed the same hypersensitive cleavage at the 5′-CG-3′ step outside the binding region (Figure 4A). These results suggest that both of the peptides have a similar DNA binding mode despite the difference in the histidine spacing.

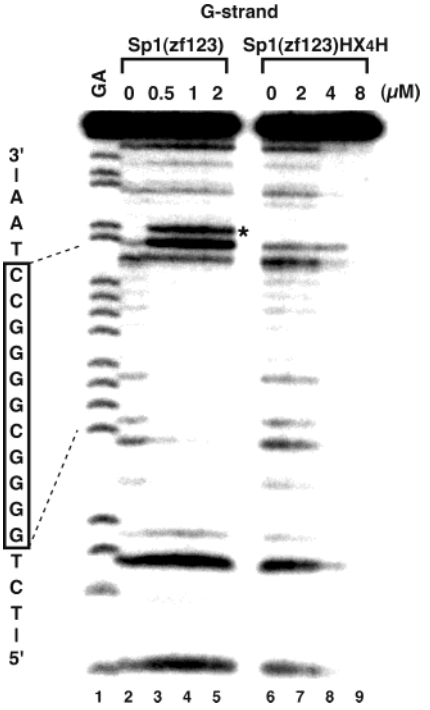

FIGURE 3: DNase I footprinting analyses of Sp1(123) and Sp1(123)HX_4H bindings to the GC box. This panel shows the results for the G strand of the GC box. The asterisk represents the enhanced site of cleavage. Lane 1 shows G + A (Maxam−Gilbert reaction products). Every peptide concentration is noted in the figure.

Detection of Specific Base Recognition by Methylation Interference Assays. Figure 5A displays the results of the methylation interference analyses for the binding of Sp1(zf123) and Sp1(zf123)HX_4H to the GC box. The extent of the interference based on a densitomeric analysis is presented in the histograms (Figure 5B). Sp1(zf123) made contact with all of the guanines at positions 1−12, although the recognition level was weak only at G7, consistent with our previous results (*13*) (Figure 5A, lanes 4, 5, 10, and 11). Sp1(zf123)HX_4H exhibited almost the same recognition patterns on the G-strand as Sp1(zf123), including the recognition of G8 and G9, which are mediated by lysine in finger 1 (Figure 5A, lanes 6 and 7) (*24*). The recognitions of G10′ and G11′ on the C-strand, which are peculiar to the N-terminal zinc finger of Sp1(zf123) (*24*), were also maintained in Sp1(zf123)HX_4H (Figure 5A, lanes 8 and 9). Consequently, each base recognition of Sp1(zf123) was not influenced by the change in the histidine spacing.

DISCUSSION

C_2H_2-type zinc fingers have certain histidine spacings from HX_3H to HX_5H, which form unique conformations because two histidine positions are restricted by the binding of a zinc ion. The CD spectra show that, regardless of sequence differences outside the histidine spacing, the ellipticities at 222 nm of HX_4H-type zinc fingers are larger than those of the HX_3H type. Our study indicates that HX_4H-type peptides have more helical content than HX_3H-type peptides. In the CD spectral results of the HX_3H-type and HX_4H-type zinc fingers of ZFY, the same tendency has been observed (*30*). This result is consistent with the fact that an HX_3H motif forms a 3_{10}-helix and an HX_4H motif forms a helical structure (*15*). Presumably, Sp1(zf23)HX_4H and GLI(zf45)HX_3H take the expected structures as a result of the mutation of the histidine spacing.

Both the Sp1-type and GLI-type peptides evidently demonstrate the reduction in the DNA binding affinity as a result of exchanging the histidine spacing. ADR1 has two

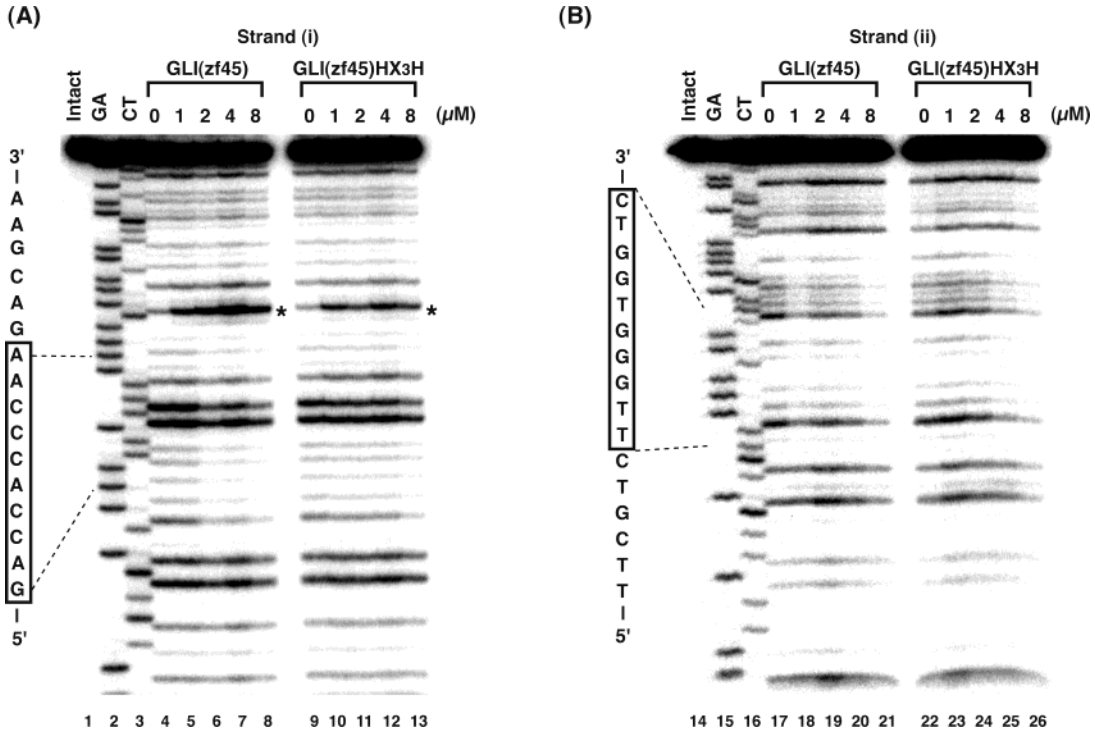

FIGURE 4: DNase I footprinting analyses of GLI(45) and GLI(45)HX_3H bindings to GLIseq. Panels A and B show the results for strands (i) and (ii), respectively. The asterisks represent the enhanced sites of cleavage. Lane 1 in panel A and lane 14 in panel B, intact DNA; lane 2 in panel A and lane 15 in panel B, G + A (Maxam−Gilbert reaction products); lane 3 in panel A and lane 16 in panel B, C + T (Maxam−Gilbert reaction products). Peptide concentration is noted in the figure.

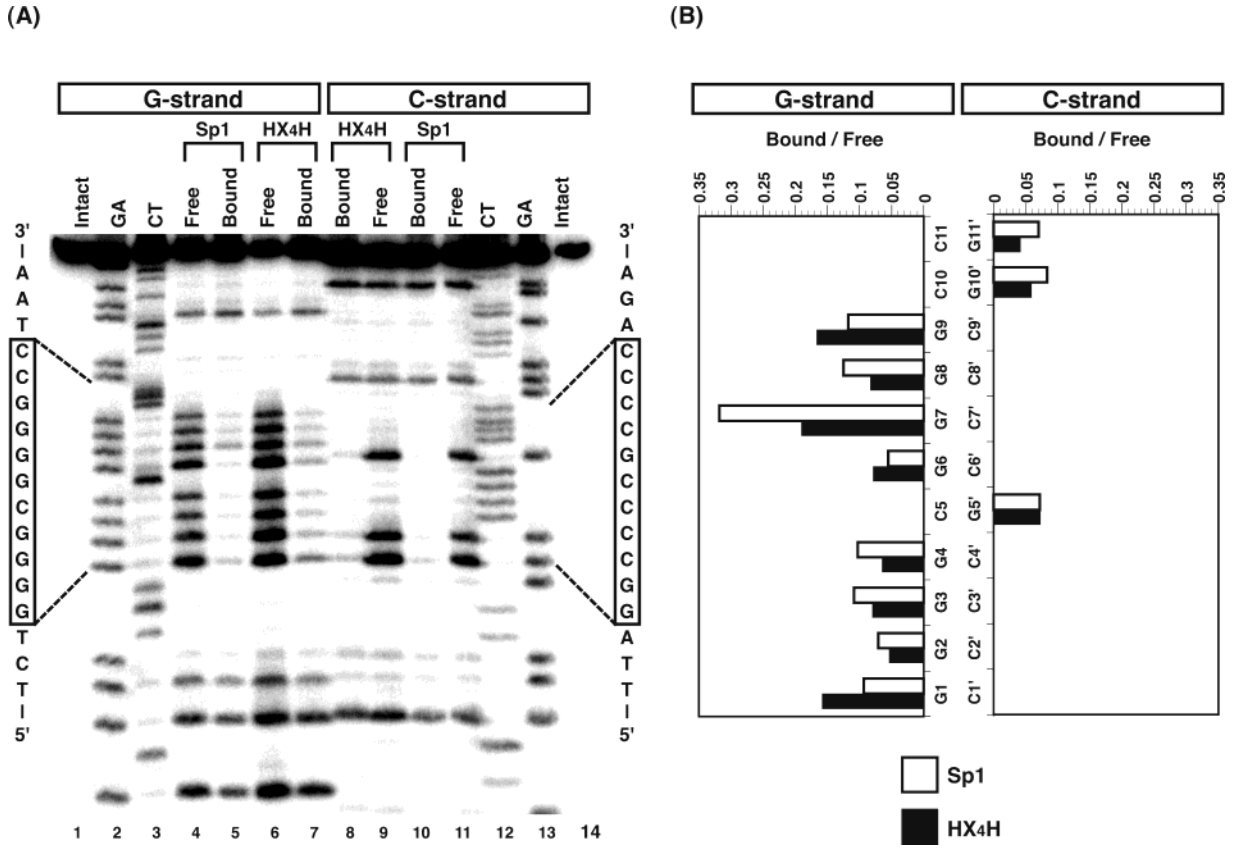

FIGURE 5: Methylation interference analyses of the binding of three-finger-type peptides of Sp1 to the GC box. Sp1 and HX_4H mean Sp1(zf123) and Sp1(zf123)HX_4H, respectively. (A) Results of autoradiograms from electrophoresis. The left (lanes 1−7) and right (lanes 8−14) panels show the results for the G- and C-strands, respectively. Lanes 1 and 14, intact DNA; lanes 2 and 13, G + A (Maxam−Gilbert reaction products); lanes 3 and 12, C + T (Maxam−Gilbert reaction products); lanes 4, 6, 9, and 11, free DNA samples; lanes 5, 7, 8, and 10, peptide-bound DNA samples. (B) Histogram showing the extent of methylation interference, which was calculated as the ratio of the cutting probabilities for the two bands (bound/free).

unique zinc fingers, consisting of HX_3H-type and HX_4H-type zinc finger motifs (*31*). In the case of ADR1, the mutation of the C-terminal zinc finger from HX_4H to HX_3H had no influence on the DNA binding affinity (*32*). In contrast to the experiments with ADR1, we changed the histidine spacing in the finger−finger connection region. On the basis of the previous structural analysis, the conformational change in the histidine spacing is local within the zinc finger domain (*15*). However, the relative orientation between continuous fingers is probably affected, leading to a decrease in the DNA binding affinity. Moreover, a drastic difference in the DNA binding affinity is observed between the Sp1-type and GLI-type peptides. A significant reduction is found in Sp1(zf23)HX_4H and Sp1(zf123)HX_4H, whereas GLI(zf45)HX_3H shows a mild reduction. These results suggest that the effect of the structural change in the histidine spacing depends on the surrounding amino acid sequences and DNA recognition mode.

From the results of DNase I footprinting analyses, GLI(zf45) binds the expected region from the binding mode of the five-finger GLI, indicating that the structure of finger 4 or finger 5 itself contributes to the extensive binding mode. GLI(zf45)HX_3H shows nearly the same binding pattern as GLI(zf45), consistent with the small difference in the DNA binding affinity. It is of particular interest that Sp1(zf123)HX_4H exhibits remarkably distinct patterns compared with Sp1(zf123). A hypersensitive cleavage is induced by the binding of the zinc finger proteins (*24*, *25*). In this study, Sp1(zf123), GLI(zf45), and GLI(zf45)HX_3H also exhibit the hypersensitive cleavage at the upstream of the binding site, suggesting that these peptides bind to the target site. On the contrary, Sp1(zf123)HX_4H shows no hypersensitive cleavage, and the protected region from DNase I digestion becomes nonspecific compared with that of Sp1(zf123). In addition, the contribution to the DNA binding affinity of lysine in finger 1 was reduced in Sp1(KA)HX_4H. These changes reveal that the specific binding mode of the Sp1 zinc finger for the GC box was lost because of the structural change derived from the histidine spacing. Despite the drastic changes in the binding affinity and the binding mode for DNA, the methylation interference analyses show that Sp1(zf123)HX_4H has almost the same base recognition patterns as Sp1(zf123). Therefore, it is thought that the base recognition mode is an intrinsic characteristic in a zinc finger domain, whereas the DNA binding affinity and the binding mode are dominated by the structure of the finger−finger connection region.

A recent structural analysis indicates that the TGEKP linker is highly conserved in C_2H_2-type zinc finger proteins and forms a helix-capping structure in binding DNA (*14*). Therefore, the stable structure of the finger−finger connection region, which contributes to the overlapping DNA recognition mode of Sp1 zinc finger, may be distorted in the Sp1 mutants with HX_4H spacings because of the structural change in the histidine spacing. This hypothesis corresponds well to the fact that the HX_3H-TGEKP linker

exists as the most common motif according to the Transcription Factor Database (*33*, *34*). On the other hand, GLI(zf45) possesses an SNEKP linker which does not form a stable structure like a TGEKP linker (*14*). Accordingly, each finger may have less structural limitations. This structural characteristic of the linker explains the slight influence of the structural change on the DNA binding affinity and the conserved extensive binding mode of the GLI zinc finger. In addition, the different linker characters are reflected in the following facts: (i) Sp1(SNE)HX_4H bound to the GC box 4.9 times more strongly than Sp1(zf123)HX_4H, and (ii) both Sp1(SNE) and Sp1(SNE)HX_4H showed the hypersensitive cleavage from DNase I to be the same as Sp1(zf123), in contrast to Sp1(zf123)HX_4H (data not shown). In ZFY and TFIIIA, the HX_4H motif and the following linker, $HX_4H\phi X_3$ (ϕ = hydrophobic residue), form a "jumping linker" which spans the minor groove (*21*, *35*). Recently, it was reported that the C-terminal histidine is unimportant for α-helix formation and DNA recognition (*36*, *37*). Therefore, the various structures in this region can be constructed by introducing unique amino acid sequences. In another case, Pabo et al. successfully used the HX_4H motif instead of the HX_3H motif in the connection of the Zif268 zinc finger to the helix region of the leucine zipper in consideration of the structural characteristic of the histidine spacing (*38*). These results strongly suggest that the histidine spacing-linker region plays an important role in DNA binding of a zinc finger peptide.

Here, we performed the exchange of the histidine spacing-linker region between Sp1 and GLI zinc fingers and showed the significant influence of this region on DNA binding affinity and DNA binding mode. Therefore, the survey of the continuous structure consisting of the histidine spacing and the following linker region is useful for regulating the cooperative recognition mode of zinc finger proteins. In addition, the selection-based design of a unique zinc finger such as GLI, which has an independent DNA recognition mode, reduces the complicated factors between successive zinc fingers. Our results provide helpful information for creation of novel zinc finger proteins recognizing more various DNA sequences.

REFERENCES

1. Pavletich, N. P., and Pabo, C. O. (1991) Zinc finger-DNA recognition: crystal structure of a Zif268-DNA complex at 2.1 Å, *Science 252*, 809−817.
2. Elrod-Erickson, M., Rould, M. A., Nekludova, L., and Pabo, C. O. (1996) Zif268 protein-DNA complex refined at 1.6 Å: a model system for understanding zinc finger-DNA interactions, *Structure 4*, 1171−1180.
3. Desjarlais, J. R., and Berg, J. M. (1992) Toward rules relating zinc finger protein sequences and DNA binding site preferences, *Proc. Natl. Acad. Sci. U.S.A. 89*, 7345−7349.
4. Desjarlais, J. R., and Berg, J. M. (1992) Redesigning the DNA-binding specificity of a zinc finger protein: a data base-guided approach, *Proteins 12*, 101−104.
5. Desjarlais, J. R., and Berg, J. M. (1992) Redesigning the DNA-binding specificity of a zinc finger protein: a data base-guided approach, *Proteins 13*, 272.
6. Desjarlais, J. R., and Berg, J. M. (1993) Use of a zinc-finger consensus sequence framework and specificity rules to design specific DNA binding proteins, *Proc. Natl. Acad. Sci. U.S.A. 90*, 2256−2260.
7. Reber, E. J., and Pabo, C. O. (1994) Zinc finger phage: affinity selection of fingers with new DNA-binding specificities, *Science 263*, 671−673.
8. Choo, Y., and Klug, A. (1994) Toward a code for the interactions of zinc fingers with DNA: selection of randomized fingers displayed on phage, *Proc. Natl. Acad. Sci. U.S.A. 91*, 11163−11167.
9. Choo, Y., and Klug, A. (1994) Selection of DNA binding sites for zinc fingers using rationally randomized DNA reveals coded interactions, *Proc. Natl. Acad. Sci. U.S.A. 91*, 11168−11172.
10. Greisman, H. A., and Pabo, C. O. (1997) A general strategy for selecting high-affinity zinc finger proteins for diverse DNA target sites, *Science 275*, 657−661.
11. Segal, D. J., and Barbas, C. F., III (2000) Design of novel sequence-specific DNA-binding proteins, *Curr. Opin. Chem. Biol. 4*, 34−39.
12. Isalan, M., Choo, Y., and Klug, A. (1997) Synergy between adjacent zinc fingers in sequence-specific DNA recognition, *Proc. Natl. Acad. Sci. U.S.A. 94*, 5617−5621.
13. Nagaoka, M., Shiraishi, Y., Uno, Y., Nomura, W., and Sugiura, Y. (2002) Interconversion between serine and aspartic acid in the alpha helix of the N-terminal zinc finger of Sp1: implication for general recognition code and for design of novel zinc finger peptide recognizing complementary strand, *Biochemistry 41*, 8819−8825.
14. Laity, J. H., Dyson, J., and Wright, P. E. (2000) DNA-induced alpha-helix capping in conserved linker sequences is a determinant of binding affinity in Cys(2)-His(2) zinc fingers, *J. Mol. Biol. 295*, 719−727.
15. Kochoyan, M., Keutmann, H. T., and Weiss, M. A. (1991) Alternating zinc fingers in the human male-associated protein ZFY: HX3H and HX4H motifs encode a local structural switch, *Biochemistry 30*, 9396−9402.
16. Omichinski, J. G., Clore, G. M., Appella, E., Sakaguchi, K., and Gronenborn, A. M. (1990) High-resolution three-dimensional structure of a single zinc finger from a human enhancer binding protein in solution, *Biochemistry 29*, 9324−9334.
17. Dynan, W. S., and Tjian, R. (1983) Isolation of transcription factors that discriminate between different promoters recognized by RNA polymerase II, *Cell 32*, 669−680.
18. Kadonaga, J. T., Jones, K. A., and Tjian, R. (1986) Promoter-specific activation of RNA polymerase II transcription by Sp1, *Trends Biochem. Sci. 11*, 20−23.
19. Narayan, V. A., Kriwacki, R. W., and Caradonna, J. P. (1997) Structures of zinc finger domains from transcription factor Sp1. Insights into sequence-specific protein-DNA recognition, *J. Biol. Chem. 272*, 7801−7809.
20. Fairall, L., Schwabe, J. W. R., Chapman, L., Finch, J. T., and Rhodes, D. (1993) The crystal structure of a two zinc-finger peptide reveals an extension to the rules for zinc-finger/DNA recognition, *Nature 366*, 483−487.
21. Nolte, R. T., Conlin, R. M., Harrison, S. C., and Brown, R. S. (1998) Differing roles for zinc fingers in DNA recognition: structure of a six-finger transcription factor IIIA complex, *Proc. Natl. Acad. Sci. U.S.A. 95*, 2938−2943.
22. Kinzler, K. W., Ruppert, S. H., Bigner, S. H., and Vogelstein, B. (1988) The GLI gene is a member of the Kruppel family of zinc finger proteins, *Nature 332*, 371−374.
23. Pavletich, N. P., and Pabo, C. O. (1993) Crystal structure of a five-finger GLI-DNA complex: new perspectives on zinc fingers, *Science 261*, 1701−1707.
24. Yokono, M., Saegusa, N., Matsushita, K., and Sugiura, Y. (1998) Unique DNA binding mode of the N-terminal zinc finger of transcription factor Sp1, *Biochemistry 37*, 6824−6832.
25. Uno, Y., Matsushita, K., Nagaoka, M., and Sugiura, Y. (2001) Finger-positional change in three zinc finger protein Sp1: influence of terminal finger in DNA recognition, *Biochemistry 40*, 1787−1795.
26. Brenowitz, M., Senear, D. F., Shea, M. A., and Ackers, G. K. (1986) Quantitative DNase footprint titration: a method for studying protein-DNA interactions, *Methods Enzymol. 130*, 132−181.
27. Wissmann, A., and Hillen, W. (1991) DNA contacts probed by modification protection and interference studies, *Methods Enzymol. 208*, 365−379.
28. Frankel, A. D., Berg, J. M., and Pabo, C. O. (1987) Metal-dependent folding of a single zinc finger from transcription factor IIIA, *Proc. Natl. Acad. Sci. U.S.A. 84*, 4841−4845.
29. Hori, Y., Suzuki, K., Okuno, Y., Nagaoka, M., Futaki, S., and Sugiura, Y. (2000) Artificial zinc finger peptide containing a novel His_4 domain, *J. Am. Chem. Soc. 122*, 7648−7653.

30. Weiss, M. A., Mason, K. A., Dahl, C. E., and Keutmann, H. T. (1990) Alternating zinc-finger motifs in the human male-associated protein ZFY, *Biochemistry 29*, 5660−5664.
31. Bernstein, B. E., Hoffman, R. C., Horvath, S., Herriott, J. R., and Klevit, R. E. (1994) Structure of a histidine-X4-histidine zinc finger domain: insights into ADR1-UAS1 protein-DNA recognition, *Biochemistry 33*, 4460−4470.
32. Cheng, C., and Young, E. T. (1995) A single amino acid substitution in zinc finger 2 of Adr1p changes its binding specificity at two positions in UAS1, *J. Mol. Biol. 251*, 1−8.
33. Ghosh, D. (1993) Status of the transcription factors database (TFD), *Nucleic Acids Res. 21*, 3117−3118.
34. Wolfe, S. A., Nekludova, L., and Pabo, C. O. (2000) DNA recognition by Cys2His2 zinc finger proteins, *Annu. Rev. Biophys. Biomol. Struct. 29*, 183−212.
35. Kochoyan, M., Havel, T. F., Nguyen, D. T., Dahl, C. E., Keutmann, H. T., and Weiss, M. A. (1991) Alternating zinc fingers in the human male associated protein ZFY: 2D NMR structure of an even finger and implications for "jumping-linker" DNA recognition, *Biochemistry 30*, 3371−3386.
36. Nomura, A., and Sugiura, Y. (2002) Contribution of individual zinc ligands to metal binding and peptide folding of zinc finger peptides, *Inorg. Chem. 41*, 3693−3698.
37. Simpson, R. J. Y., Cram, E. D., Czolij, R., Matthews, J. M., Crossley, M., and Machay J. P. (2003) CCHX zinc finger derivatives retain the ability to bind Zn(II) and mediate protein-DNA interactions, *J. Biol. Chem. 278*, 28011−28018.
38. Wolfe, S. A., Ramm, E. I., and Pabo, C. O. (2000) Combining structure-based design with phage display to create new Cys(2)-His(2) zinc finger dimers, *Structure 8*, 739−750.

BI035999S